Special Proceedings: ISBN #: 978-81-950383-2-9
25th Annual Conference, 15-17 February 2023; pp 79-92

A New Development of Threshold Selection in Extreme Value Theory

K. M. Sakthivel and V. Nandhini
Department of Statistics, Bharathiar University, Coimbatore, Tamil Nadu.

Received: 15 June 2023; Revised: 21 July 2023; Accepted: 25 July 2023

Abstract

Extreme value theory addresses the stochastic behavior of the extreme values in a process. There are two important methods used in modeling extreme value analysis and they are threshold selection and block maxima techniques. The threshold selection is important in many aspects of statistical inference of extreme or rare events because they use data more effectively than block maxima techniques. The inference derived from the threshold method mainly depends on the selection of the optimum threshold and it can be determined approximately using the parameter stability plot and mean residual life plot. Since the extreme value theory considers only extreme values in the given set of data. So there is an unresolved issue in determining the optimal threshold while using the peaks over threshold technique. Further exceedances above a high threshold have been shown to asymptotically follow the generalized Pareto distribution under the usual circumstances. In this paper, a new development in threshold selection technique is discussed in detail for modeling extreme values along with real-life applications.

Key words: Extremes; Tail behavior; Peaks over threshold; Block maxima; Return level.

AMS Subject Classifications: 62E20, 62M10.

1. Introduction

Extreme Value Theory (EVT) is a specialized field of statistics that provides methodologies and tools for the study and estimation of probabilities of events that have not been previously observed or rare events. Because these extreme events are sparse, extrapolation beyond the observed levels is required for estimation. EVT is designed explicitly for such extrapolation and utilizes asymptotic analyses as the foundation of extreme value models. This theory indicates that extreme value estimation is only related to the tail of the probabilistic distribution. The objective of extreme value analysis is to determine how likely it is that certain events will occur that are the least likely to have previously been observed. The techniques and models have been developed to describe the tails of the data and estimate the probabilities of extreme events.

Correponding Author: K.M. Sakthivel
Email: sakthithebest@buc.edu.in

In the literature on extreme value theory, several researchers have applied these special techniques in different real scenarios of the countries to come up with several estimates about extreme events. EVT has two commonly used approaches block maxima and peaks over threshold approaches. In block maxima (BM), the peak value of each block is considered an extreme value, and block sizes are usually taken on year. But in some cases, the block size may vary depending on the nature of the study areas. Such extreme values from block maxima also known as annual or cluster maxima, these values can be modeled using the generalized extreme value (GEV) distribution which came from the first theorem of EVT that is Fisher Tippett Gendenko theorem (1928). The peaks over a threshold (PoT) method is popular in the extreme value analysis because it prefixes the threshold for the whole observations, the values above the threshold are considered as the extreme values of the specific cases. The generalized Pareto (GP) distribution can be used to model the extreme value sequence from the PoT method. This GP distribution originated from the second theorem of EVT called the Pickands-Balkema-De Haan theorem (1975). However, some other methods can also be available, r-largest order statistic with GEV and point process (PP) with GP approaches.

So, according to Coles (2001), EVT can simulate the stochastic nature of processes involving events of unusually high or low intensity. Pickands (1975) proposed a method for making decisions about the upper tail of the distribution. It can be used to predict the likelihood that future extremely large observations. And GP distribution can be introduced to model extreme values. Smith (1989) proposed specific modifications based on the point-process view of high-level exceedances via a clustering approach with ozone data analysis. Davison and Smith (1990) talked about modeling the sizes and occurrences of exceedances in order to analyze data extremes. Katz *et al.* (2002) explained the evolution of extremes, which includes the development of a point process framework that incorporates block maxima and PoT techniques. Sanders (2005) shows the modeling of extreme events is becoming of increased importance to actuaries. Cooley (2011) investigated the definitions of return period and return level given by Olsen *et al* (1998) the m-year return level was the level for which the expected waiting time until the exceedances in m-years and Parey *et al.* (2007) was the m-year return level as the level for which the expected number of events in an m-year period is one can be considered under the nonstationary setting. Deidda (2010) introduced a multiple threshold method (MTM) to infer the parametes by using excess over the threshold applying againt the concepts of parameters threshold invariance, and also discussed the supremacy of the MTM fit against the single threshod fit. Scarrot and Mac-Donald (2012) developed the parameter stability plot, with an emphasis on estimating the shape and scale parameters in order to determine an appropriate threshold. De Zea *et al.* (2012) employed the PoT method to model the sample of excesses above a sufficiently high value of total cholesterol level of patients. Bader *et al.* (2018) developed the automated sequential threshold via ordered goodness of fit tests with adjustment for false discovery rate. Roux *et al.* (2020) studied the trends in 50 years' return levels of the ground snow loads using non-stationary extreme value models for the French Alps with its building standards. Hesarkazzazi *et al.* (2021) investigated the process of non-stationary annual maxima of river peak flow in northwest England and a regression model for the location parameter of the generalized logistic distribution (GLO) was also constructed. Tanprayoon *et al.* (2023) proposed a new Gompertz-generalized extreme value distribution for extreme value analysis and return-level estimation of the extreme rainfall.

In some sectors of science and technology, the extreme values of significant variables have special meanings and importance. The extreme value theory has recently been applied in terrestrial and solar climatology. The sunspot number series, which was recorded from 1818 to 2022, is used to study extreme values of solar activity. The observations of daily sunspot numbers have been collected from the database of Solar Influences Data Analysis Center (SIDC) - the solar physics research department of the Royal Observatory of Belgium. Sunspots are dark, planet-sized areas that appear on the surface of the sun. Sunspots are magnetic regions on the sun with magnetic field strengths thousands of times greater than the Earth's magnetic field. Sunspots appear in active regions, usually in opposite magnetic polarity pairs. Their number varies with the roughly 11-year solar cycle. Sunspot magnetic fields are extremely strong, keeping heat away from these regions of the sun's surface. The active region is a temporary region with a strong and complex magnetic field in the sun. They are often associated with sunspots and can be a source of eruptions like solar flares and coronal mass ejections (CMEs). Solar flares are a burst of energy caused by the tangling, crossing, or reorganization of magnetic field lines near sunspots. The variation in the number of sunspots and solar activity are closely related. Because solar activity can have an impact on Earth, scientists closely monitor it every day.

When sunspot counts are high, the sun is very active, and the peak in the sunspot count is referred to as a solar maximum, whereas a period when fewer or no sunspots appear is referred to as a solar minimum. Sunspots can cause geomagnetic storms in the Earth's magnetosphere. When sunspot numbers are at their peak during the solar maximum period, the sun emits more radiation than usual. A solar flare emits a large amount of radiation into the universe. Intense solar flares can interfere with radio waves, telecommunications, the electric power grid, and satellite navigation by releasing radiation that interferes with these systems. Therefore, due to the high number of sunspots in the sun's photosphere, there is a chance that solar flares and coronal mass ejections will appear. In this case, extreme value analysis is essential to find out the extreme occurrences of the sunspot number during the solar maximum period of this current solar cycle. The extreme values of previous events of sunspots decide the behavior of the future event of the study. Acero *et al.* (2017) used the block maxima method with the GEV distribution for modeling the maximum values of the sunspot numbers at yearly, monthly, and daily scales for each solar cycle and the PoT approach only for daily scales, which takes into account all sunspot numbers that exceed a predefined upper threshold and can be modeled using the GP distribution. The return levels were predicted for 10 (110 years), 50 (550 years), and 100 (1100 years) solar cycles. Elvidge *et al.* (2018) used EVT to investigate the likelihood of extreme solar flares with both GOES X-ray flux data and Kepler mission data.

In this paper, we are interested to develop a new threshold selection methodology that is superior to the existing PoT method. The sunspot numbers data set is used for this theory to estimate the return levels associated with the return periods, as well as to calculate the probability of exceedances. It is therefore essential to study and model these extremes to make accurate prognostications of return levels. As a result, new approaches for predicting extreme occurrences can be developed and they can be modeled with GP distribution in application to sunspot number series. This paper has been divided into five sections. Following this introduction, Section 2 presents research materials and methodologies, Section 3 performs preliminary data analysis, Section 4 describes the interpretation of the results, and Section 5 shows a summary and conclusion.

2. Methodology

In this section, we will discuss the procedures for both the traditional and proposed threshold selection methodologies for segregating extreme values from a series of observations. Those extreme values can be modeled with appropriate distribution to predict future events by the return period concept for this case.

2.1. Peaks over threshold

The PoT method were created by Pickands (1975) and it concentrates on observations that seem to go above a high threshold. The PoT with GP distribution can be used to avoid the problem of data waste, which is a common problem with the block maxima method. However, determining an appropriate threshold is an inherent problem specifically. If the threshold has been too low, the tail will satisfy the less convergence criterion, causing a large bias and an incorrect result. If the threshold is too high, however, very few values above the threshold will result in high variance and imprecise results. Thus, selecting an appropriate threshold necessitates balancing the bias and the variance.

The GP distribution has a continuous range of possible shapes, including special cases of the exponential and Pareto distributions. We can use either of these to model a specific set of exceedances. The two-parameter GP distribution with shape parameter ξ and scale parameter σ has the following representation.

The cumulative distribution function of the two-parameter GP distribution with a shape parameter ξ, the scale parameter σ is given by

$$F(x|\sigma,\xi) = \begin{cases} 1-[1+\xi(\frac{x}{\sigma})]^{-\frac{1}{\xi}}; & \text{for} \quad \xi \neq 0 \\ 1-\exp\{-[\frac{x}{\sigma}]\}; & \text{for} \quad \xi = 0 \end{cases} \tag{1}$$

where, $x > 0$ when $\xi > 0$ and $0 \leq x \leq -\sigma/\xi$ when $\xi \leq 0$. and corresponding probability density function is

$$f(x|\sigma,\xi) = \begin{cases} \frac{1}{\sigma}[1+\xi(\frac{x}{\sigma})]^{-\frac{\xi-1}{\xi}}; & \text{for} \quad \xi \neq 0 \\ \frac{1}{\sigma}\exp\{-[\frac{x}{\sigma}]\}; & \text{for} \quad \xi = 0 \end{cases} \tag{2}$$

If $\xi > 0$, the above equation reduces to Pareto distribution, which is a heavy-tailed distribution. If $\xi = 0$ it is reduced to the exponential distribution. If $\xi < 0$ it is simply to obtain light-tailed distribution with finite endpoints such as short-tailed Pareto or uniform distribution. The mean and variance of a distribution is given by

$$E(x|\sigma,\xi) = \frac{\sigma}{1+\xi} \text{ and}$$

$$V(x|\sigma,\xi) = \frac{\sigma^2}{(1+\xi)^2(2\xi+1)} \text{ exists if } \xi > -1, \xi > -\tfrac{1}{2} \text{ respectively.}$$

2.2. Reduced threshold - a new approach

The newly developed reduced threshold (RT) method divides the entire set of observations into equal-sized non-overlapping periods and focuses on the extreme values in these periods. These extreme values are taken into account when determining the threshold point. When compared to the traditional BM and PoT method, the extreme values above this particular threshold point are considered special extreme values. There are 'm' numbers of observations in each of the 'n' periods. Therefore there is $m \times n$ number of total observations.

Let us consider the blocks B_{ij} for $j = 1, 2, ..., k; i = 1, 2, ..., n$, where i represent the position of each block consisting of j is the number of independent and identically distributed observations. The maximum values of every block are considered extreme values which are represented as the following sequence,

$$Z_i = \{z_1, z_2, ..., z_k\}; \text{for every } i = 1, 2, ..., n$$

Let Z_i be the sequence of iid random variables with CDF $F(z)$ and let ξ_p denoted by p^{th} quantile of F, so that $\xi_p = inf\{z|F(z) \geq p\}$. The p^{th} quantile is defined as $F(\xi_p) = p$. Let $Q_p = Z_{(i)\lfloor np \rfloor:n}$ denote a sample p^{th} quantile. Here $\lfloor np \rfloor$ denotes the greater integer $\leq np$. The weighted average of the distribution's median and quantiles Q_p and Q_{1-p} for $p \in (0, 1/2)$ is known as the "Trimean estimator", such that

$$\hat{\tau} = \frac{\alpha}{2} Q_p + (1 - \alpha) Q_{1/2} + \frac{\alpha}{2} Q_{1-p} \tag{3}$$

The weights for the two quantiles are the same for Q_p and Q_{1-p}, and the weight $\alpha \in [0, 1]$. The Tukey's Trimean estimator is obtained by taking $\alpha = \frac{1}{2}$ and $p = \frac{1}{4}$ in the above equation and it is a special case of the Trimean estimators. It can be defined as

$$\hat{\tau}_{TM} = \tfrac{1}{4} Q_{1/4} + \tfrac{1}{2} Q_{1/2} + \tfrac{1}{4} Q_{3/4} \tag{4}$$

The threshohd u^* can be obtained by $\hat{\tau}_{TM}$ and first quartile of the extreme value sequence of iid's.

$$u^* = \frac{1}{2}[\hat{\tau}_{TM} + Q_{1/4}] \tag{5}$$

when the values exceed the threshold u then as the special extreme values denote Z_s^* for $s = 1, 2, ..., k$.

$$Z_s^* = \{z_1^*, z_2^*, ..., z_k^*\}, \text{for} Z_s^* \geq u, Z_s^* \neq Z_i. \tag{6}$$

These special extreme values from the RT method can be modeled with generalized Pareto distribution.

2.3. Tail dependence and declustering

In stationary sequences, extreme values can occur in clusters. The first step in making inferences is to identify clusters in the data, which is accomplished through the declustering process. Declustering could be effective at screening the dependent observation to a set of threshold exceedances. The empirical rule can be used to define the cluster of exceedances, and the maximum excess in each cluster can be determined. Runs and interval methods can be used in such cases to separate the clusters and estimate the extremal index. The extremal index θ is a measure of the degree of local dependence in the extremes of a stationary process it ranges from 0 to 1, that is $\theta \in [0, 1]$, where to imply some dependence. When θ the value decreases there is evidence for greater dependence. In Runs declustering, a run length (the minimum gap between clusters) 'r' can be fixed to choose the cluster, and the extremes are separated by fewer than 'r'-non extremes belonging to the same cluster. The choice of 'r' is critical because too small a value causes the problem of independence being unrealistic for nearby clusters, while too large a value causes the concatenation of clusters that could reasonably be considered independent, potentially resulting in the loss of valuable data.

2.4. Return periods and return levels

The return levels and return periods, which are crucial for the prediction of extreme events, can be discovered when the distribution is fitted. The return level predicts that the event will occur at least once over the following 't' years. For the GP model, the return level is given x_q which defines the extreme level that exceeds at least once every 'q' observations. The return period of the GP model is

$$P(X > x|X > u) = [1 + \xi(\tfrac{x-u}{\sigma})]^{-\frac{1}{\xi}}$$

Let $\xi_u = P(X > u) = r/n$, where r is the number of upper order values exceeding the threshold u, and n is the number of years of records then the return period can be simplified as follows

$$P(X > x) = \left[1 + \xi(\tfrac{x-u}{\sigma})\right]^{-\frac{1}{\xi}}$$

This implies that the data points exceed once in every 'm' series of observations on average can be determined as

$$\xi_u \left[1 + \xi(\tfrac{x-u}{\sigma})\right]^{-\frac{1}{\xi}} = \frac{1}{m}$$

Finally, the m-year return level for GPD is given by

$$x_m = \begin{cases} u - \frac{\sigma}{\xi}[(m\xi_u)^{\xi} - 1]; & \xi \neq 0 \\ u - \sigma \log[m\xi_u]; & \xi = 0 \end{cases} \tag{7}$$

where x_m is the return level associated with the return period $q = 1/m$.

The return level is the interesting final product of the extreme value analysis in the prediction of tail probabilities. Therefore, when 'm' should be large enough, the return level x_m exceeds the threshold 'u'.

3. Application

3.1. Data source

The daily sunspot numbers dataset spans 205 years which is more than two centuries, beginning in January 1818 and ending in December 2022. The sunspot number daily of observations have been collected from the database of Solar Influences Data Analysis Center (SIDC) - the solar physics research department of the Royal Observatory of Belgium. It is publicly available on SIDC's Sunspot Index and Long-term Solar Observations (SILSO) website.

3.2. Data modeling and analysis

The excess over the threshold technique can be used to separate the extreme sunspot number from the non-extremes by selecting the appropriate threshold. The two approaches discussed above can be used to identify extreme sunspots, and the exceedances can be modeled with an appropriate distribution, which can then be used to estimate the return levels. The PoT approach takes into consideration only those sample sunspot number values that are significantly larger than a predetermined threshold u. The scale parameter of the distribution can be modified that is $\sigma^{*}= \sigma - \xi u$ against the threshold u which has been shown in the modified scale parameter threshold stability plot in Figure 1. In this figure,

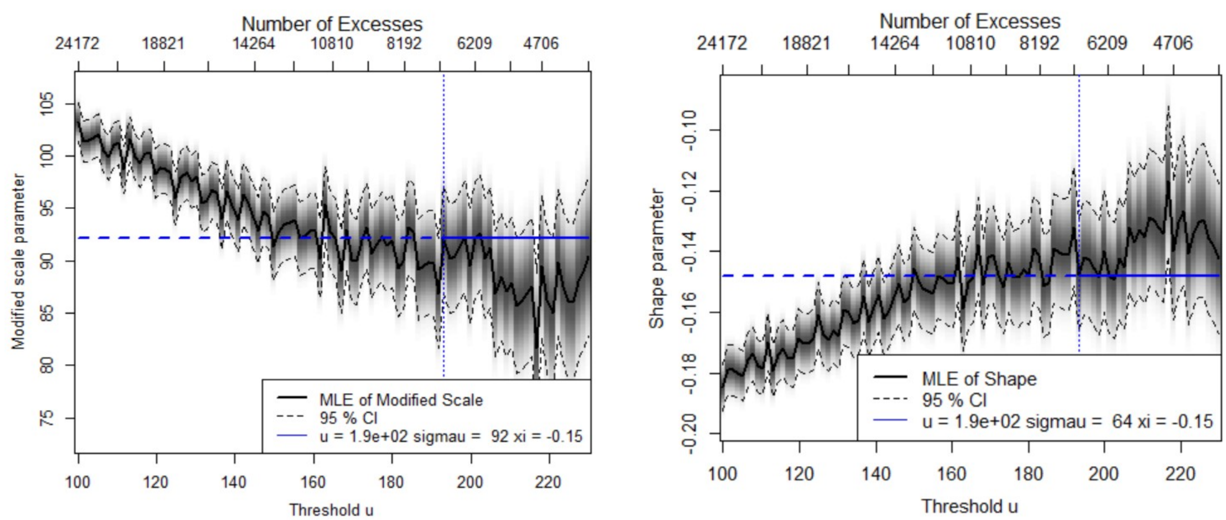

(a) Modified scale parameter **(b) Shape parameter**

Figure 1: Threshold stability plot

the dark black line represents the estimated parameter value and the shaded area describes its confidence level for $u = 190$, the vertical line represents the threshold value, and the horizontal line shows the estimated parameter value, the threshold stability plot can be used to determine an appropriate threshold. The mean residual life (MRL) plot is another alternative way of choosing an appropriate value of the threshold which is shown in Figure 2. It plots an average value over a given threshold for a series of thresholds. A mean excess plot with a downward-sloping line indicates thin-tailed behavior. The MRL plot shows the mean number of excesses over the threshold u, in between a confidence interval (approx 95%). We look for approximate linearity (from the lowest possible threshold) whilst keeping in between the confidence bounds.

The RT is a new technique for determining an adaptive threshold u, particularly for dependence sequences. In this series of sunspot numbers, the RT approach uses trimean $\hat{\tau}_{TM}$

and $Q_{1/4}$ finds the threshold u^* from the yearly maximum extreme value series, sometimes also known as annual maxima. Since maximum values of sunspot numbers are grouped into clusters, one should expect that there may be several consecutive days with the maximum exceeding the threshold. To avoid short-term dependencies in the time series, these expected clusters of exceedances would necessitate the use of a declustering procedure to identify approximately independent clusters of extreme observations within the sample.

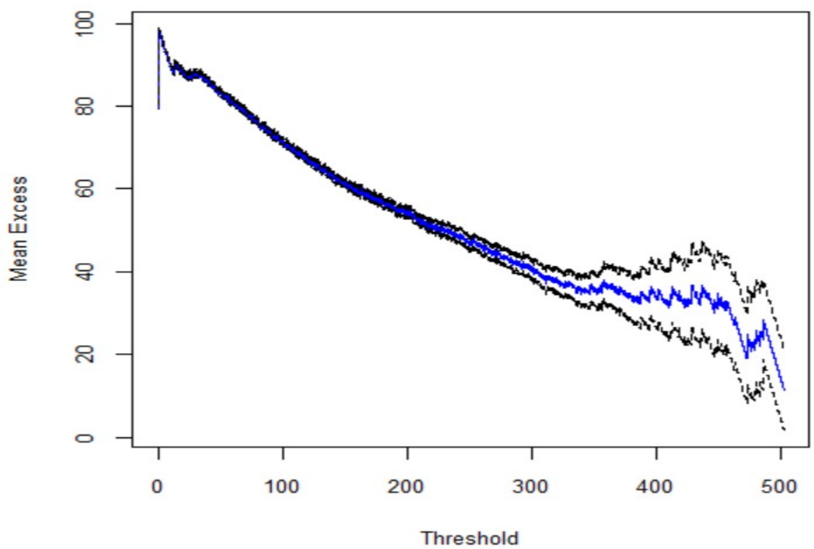

Figure 2: Mean residual life plot

The runs declustering process involves grouping exceedances into the same cluster if their distance from one another is less than the predetermined run length r. The extremal index for sunspot number from PoT threshold 190 is 0.01399, demonstrating the sequence's strong dependence. When 103 clusters are above the threshold and the appropriate run length is r=69, the maximum values of each cluster are regarded as extreme values. The weak dependence in the sequence is indicated by the associated extremal index, which is 0.8844 respectively. Figure 3 depicts the declustered sunspot numbers data using the runs method of declustering. The horizontal line in the figure represents the u=190 line over the years, and the values above the threshold are considered extreme values. These values are declustered to form 103 clusters, from which the higher order values for this study are taken. The new declustering series data can be modeled using the GP distribution. Maximum likelihood estimation is used to estimate the parameters. The value of the parameter estimates with its standard error for scale $\sigma = 74.0544(11.7214)$ and shape $\xi = 0.0215(0.1238)$. The variance-covariance matrix of the parameters for the peaks over threshold associated with GP is given as follows

$$CV = \begin{bmatrix} 137.3902 & -1.12069 \\ -1.12069 & 0.01534 \end{bmatrix}$$

The diagonals of the matrix are the variance for the fitted model. The 95% CI for the parameters scale has (51.0811, 97.0279) and shape has (-0.22132, 0.2642) respectively.

Figure 4 depicts the declustered sunspot numbers data using the runs method of declustering. The horizontal line in the figure represents the u^*=162 line over the years and

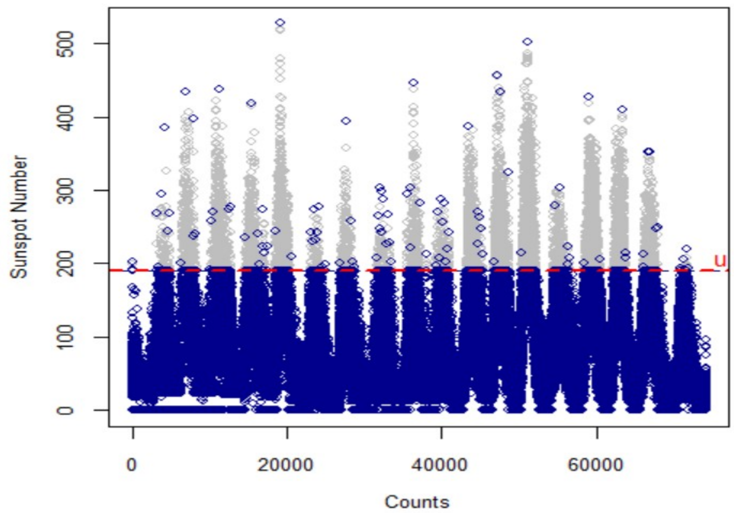

Figure 3: Declustering series plot for PoT

highlighted values above the threshold are considered extreme values of each cluster. The extremal index for RT is 0.01108 for the obtained threshold, demonstrating the severe dependence in sequence. In this case, the appropriate run length is r=55, with 126 clusters above the threshold, and the maximum values of each cluster are considered to be the extreme values. The associated extremal index is 0.9023 which describes the weak dependence in the sequence. The GP distribution can be used to model the new

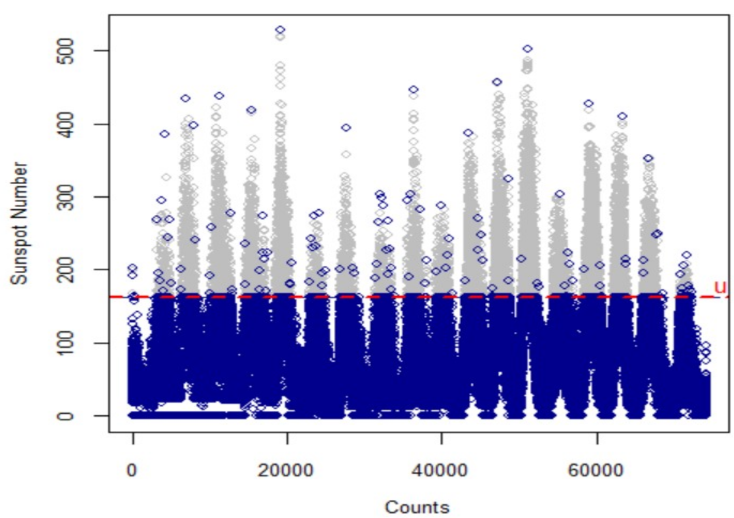

Figure 4: Declustering series plot for RT

declustering series data. The parameters are estimated using the maximum likelihood estimation. The value of the parameter estimates with its standard error for scale $\sigma = 62.70(9.3351)$ and shape $\xi = 0.1427(0.1202)$ respectively. The variance-covariance matrix of the parameters for the reduced threshold associated with GP is given by

$$CV = \begin{bmatrix} 90.0442 & -0.81475 \\ -0.81475 & 0.01367 \end{bmatrix}$$

The diagonals of the matrix are the variance of the parameters for the fitted model. The estimate $\xi > 0$ indicates that its domain of attraction is the Pareto (heavy-tailed) distribution. The 95% CI for the parameters scale has (44.2846, 80.8806) and the shape has (-0.09223, 0.38014) respectively.

4. Model diagnostics and return levels

In this section, we examine the results of two models: peaks over the threshold with GP distribution and reduced threshold with GP distribution. The model is chosen using the goodness of fit tests such as Anderson-Darling, Cramer-von Mises, and Kolmogorov-Smirnov, and the results are shown in Table 1. The models are ranked based on their performance, and return levels for various return periods are computed. Table 1 presents the goodness of fit test statistic as well as the p-value for the models under consideration in this study. The model with the least statistic is ranked with the lowest value in the range for each measure; among these, the reduced threshold-GP distribution shows a reasonable fit for this dataset.

Table 1: Results of goodness of fit tests

Models	A_n^2 (**p-value**)	W_n^2 (**p-value**)	D_n (**p-value**)
PoT-GP	0.5664 (0.6800)	0.0603 (0.8133)	0.0587 (0.8695)
RT-GP	0.4961 (0.7504)	0.0392 (0.9381)	0.0469 (0.9444)

Table 2: Estimated return levels with 95% confidence interval

RP(yr)	**PoT-GP**	**RT-GP**
2023	139 (115, 163)	133 (117, 148)
2024	190 (176, 205)	175 (164, 186)
2025	221 (204, 237)	202 (188, 216)
2026	242 (223, 261)	222 (205, 239)

Table 2, above shows the estimated return level of the sunspot numbers for the maximum period of the current 25^{th} solar cycle, from 2023 to 2026. The solar maximum is expected to occur between 2024 and 2026. According to a NASA report, scientists anticipate a rise in solar activity leading up to the next maximum, which could occur in 2025. Usually, the maximum period is unknown because no one can predict it precisely. No one knows when the sun's polarities change precisely; it cannot happen at a precise time, but it does happen over an approximate period. We predicted the sunspot number for 2023 to 2026 as well, because the exact maximum period has not been exactly predicted by scientists, if the maximum period of the current cycle will extend to 2026, this prediction may be useful.

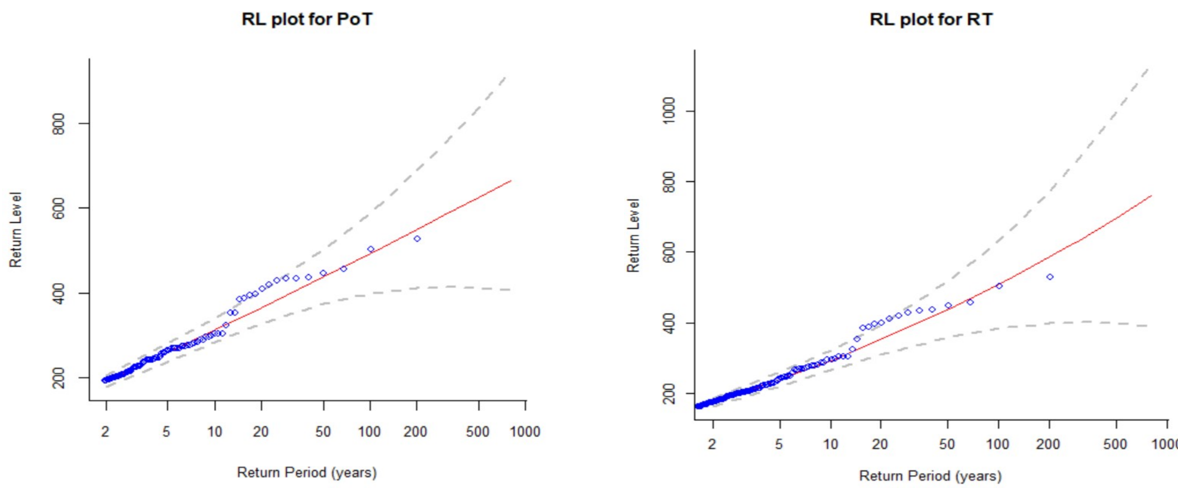

Figure 5: Return Level Plot for PoT and RT

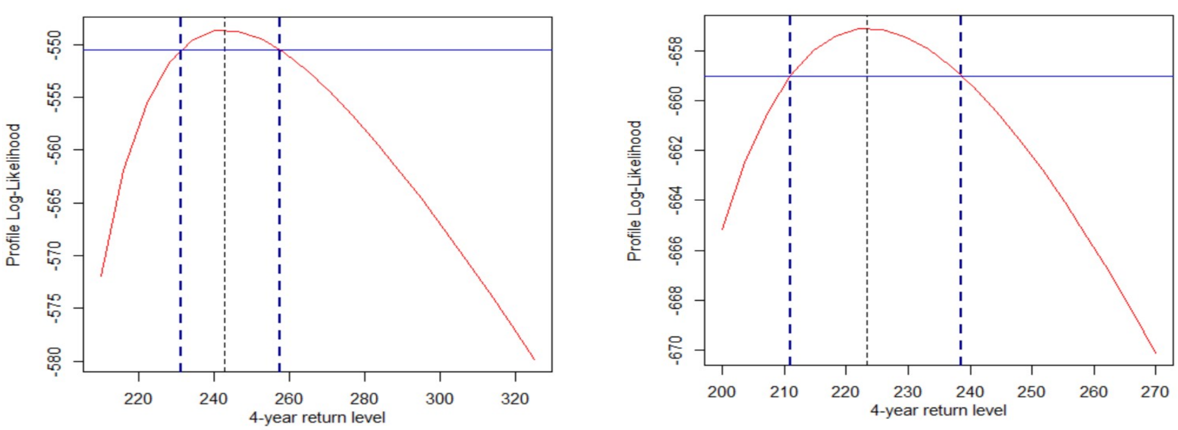

Figure 6: Profile likelihood plot for PoT and RT

The return level can be estimated by the delta method, for PoT is 242 with a 95% confidence interval is (223, 262), for RT is 223 with a 95% confidence interval is (206, 240) respectively. The return levels are graphically represented in Figure 5; it shows the estimated values associated with its confidence interval. When the time increases the estimated values of the sunspot numbers of the solar maximum period also increase with its confidence limits. The return levels can also be obtained using the profile likelihood method, we get the estimated value of the 4-year return level for the PoT method is 242 and its approximate 95% confidence interval is (223, 262), the estimated value of the 4-year return level for RT method is 223 and its approximate 95% confidence interval is (211, 238). Figure 6 displays the profile likelihood for the 4-year return level. Because the profile likelihood crosses both the blue vertical dashed and horizontal solid lines, the resulting intervals are believable. We select the RT method because it provides a better fit for the extreme values than the PoT method. The estimated return levels of sunspot numbers based on the RT method are thus taken into account.

5. Summary and conclusions

This study developed a new reduced threshold method for selecting a suitable threshold, and the generalized Pareto distribution can be used to model the extreme values. In the context of extreme value analysis, we applied the peaks over threshold and reduced threshold techniques to the sunspot number series from 1818 to 2022 years to establish the decision threshold. A generalized Pareto with shape and scale parameters can be used to model exceedances above the threshold. The behavior of the extreme value series is described by the estimated extreme value index. The shape parameter of the aforementioned two methods are positive in this situation, indicating that the distribution is heavily tailed according to the series. This study focuses on the maximum period of sunspots in the solar cycle because there is a possibility of solar flares and CMEs occurring during that period. The m-year return levels were estimated for the 25^{th} solar cycle's maximum periods, such as 2023-2026. This prediction could be helping to determine the next maximal event. We will discuss only the rare event rather than all occurrences because it will be more useful to observe the tail behavior with less probability. In this study, we explore how the peaks over threshold and the reduced threshold can be used to estimate the model's tail parameters. Among these, our suggested model has the narrowest return level confidence interval. The goodness of fit test can be used in conjunction with this study to evaluate the models and precision.

References

Acero, F. J., Carrasco, V. M. S., Gallego, M. C., García, J. A., and Vaquero, J. M. (2017). Extreme value theory and the new sunspot number series. *The Astrophysical Journal*, **839**, 98.

Acero, F. J., Gallego, M. C., García, J. A., Usoskin, I. G., and Vaquero, J. M. (2018). Extreme value theory applied to the millennial sunspot number series. *The Astrophysical Journal*, **853**, 80.

Bader, B., Yan, J., and Zhang, X. (2018). Automated threshold selection for extreme value analysis via ordered goodness-of-fit tests with adjustment for false discovery rate. *Annals of Applied Statistics*, **12**, 310–329.

Coles, S., Bawa, J., Trenner, L., and Dorazio, P. (2001). An introduction to statistical modeling of extreme values. *Springer.*

Cooley, D. (2012). Return periods and return levels under climate change. *In Extremes in a changing climate: Detection, analysis and uncertainty, Dordrecht: Springer Netherlands.*, **839**, 97–114.

Davison, A. C., and Smith, R. L. (1990). Models for exceedances over high thresholds. *Journal of the Royal Statistical Society: Series B (Methodological)*, **52**, 393–425.

De Haan, L. (1976). Sample extremes: An elementary introduction. *Statistica Neerlandica*, **30**, 161–172.

Deidda, R. (2010). A multiple threshold method for fitting the generalized Pareto distribution to rainfall time series. *Hydrology and Earth System Sciences*, **14**, 2559–2575.

De Zea Bermudez, P., and Mendes, Z. (2012). Extreme value theory in medical sciences: Modeling total high cholesterol levels. *Journal of Statistical Theory and Practice*, **6**, 468–491.

Elvidge, S. and Angling, M. J. (2018). Using extreme value theory for determining the probability of Carrington-like solar flares. *Space Weather*, **16**, 417–421.

Fisher, R. A. and Tippett, L. H. C. (1928). Limiting forms of the frequency distribution of the largest or smallest member of a sample. *In Mathematical proceedings of the Cambridge philosophical society, Cambridge University Press.*, **24**, 180–190.

Gumbel, E. J. (1958). Statistics of Extremes. *Columbia University Press, New York.*

Hamdi, Y., Duluc, C. M., and Rebour, V. (2018). Temperature extremes: estimation of non-stationary return levels and associated uncertainties. *Atmosphere*, **9**, 129.

Hall, P. and Weissman, I. (1997). On the estimation of extreme tail probabilities. *Annals of Statistics*, 1311–1326.

Hesarkazzazi, S., Arabzadeh, R., Hajibabaei, M., Rauch, W., Kjeldsen, T. R., Prosdocimi, I., ... and Sitzenfrei, R. (2021). Stationary vs non-stationary modelling of flood frequency distribution across northwest England. *Hydrological Sciences Journal*, **66**, 729–744.

Hill, B. M. (1975). A simple general approach to inference about the tail of a distribution. *The Annals of Statistics*, **3**, 1163–1174.

Hosking, J. R. and Wallis, J. R. (1987). Parameter and quantile estimation for the generalized Pareto distribution. *Technometrics*, **29**, 339–349.

Hosking, J. R. M., Wallis, J. R., and Wood, E. F. Estimation of the generalized extreme-value distribution by the method of probability-weighted moments. *Technometrics*, **27**, 251–261.

Katz, R. W., Parlange, M. B., and Naveau, P. (2002). Statistics of extremes in hydrology. *Advances in Water Resources*, **25**, 1287–1304.

Leadbetter, M. R. and Rootzen, H. (1988). Extremal theory for stochastic processes. *The Annals of Probability*, **16**, 431–478.

Le Roux, E., Evin, G., Eckert, N., Blanchet, J., and Morin, S. (2020) Non-stationary extreme value analysis of ground snow loads in the French Alps: a comparison with building standards. *Natural Hazards and Earth System Sciences*, **20**, 2961–2977.

Olsen, J. R., Lambert, J. H., and Haimes, Y. Y. (1998). Risk of extreme events under nonstationary conditions. *Risk Analysis*, **18**, 497–510.

Parey, S., Hoang, T. T. H., and Dacunha-Castelle, D. (2010). Different ways to compute temperature return levels in the climate change context. *Environmetrics*, **21**, 698–718.

Parey, S., Malek, F., Laurent, C., and Dacunha-Castelle, D. (2007). Trends and climate evolution: Statistical approach for very high temperatures in France. *Climatic Change*, **81**, 331–352.

Pickands III, J. (1975). Statistical inference using extreme order statistics. *The Annals of Statistics*, **3**, 119–131.

Smith, R. L. (1989). Extreme value analysis of environmental time series: an application to trend detection in ground-level ozone. *Statistical Science*, **4**, 367–377.

Sanders, D. E. A. (2005). The modelling of extreme events. *British Actuarial Journal*, **11**, 519–557.

Scarrott, C. and MacDonald, A. (2012). A review of extreme value threshold estimation and uncertainty quantification. *REVSTAT-Statistical Journal*, **10**, 33–60.

Soukissian, T. H. and Arapi, P. M. (2011). The effect of declustering in the r-largest maxima model for the estimation of Hs-design values. *The Open Ocean Engineering Journal*, **4**, 34–43.

Shaikh, Y. H., Khan, A. R., Iqbal, M. I., Behere, S. H., and Bagare, S. P. (2008). Sunspots data analysis using time series. *Fractals*, **16**, 259–265.

Tawn, J. A. (1988). An extreme-value theory model for dependent observations. *Journal of Hydrology*, **101**, 227–250.

Tanprayoon, E., Tonggumnead, U., and Aryuyuen, S. (2023). A New Extension of Generalized Extreme Value Distribution: Extreme Value Analysis and Return Level Estimation of the Rainfall Data. *Trends in Sciences*, **20**, 4034–4034.